Shortwave Cloud Radiative Forcing: Magnitude, Biases, and Uncertainties

A. P. Trishchenko and Z. Li
Canada Centre for Remote Sensing
Ottawa, Ontario, Canada

Introduction

Cloud radiative forcing (CRF) has been employed widely in studying the effects of cloud on the earth's radiation budget. By its definition, CRF denotes the influence of cloud only on radiative fluxes. However, in practice, observational determination of CRF is fraught with uncertainties due to variations in many factors other than cloud. The most notable are aerosol, water vapor, data sampling effects, and uncertainty associated with the magnitude of surface albedo. Here, we study the influence of these parameters on the derivation of CRF by means of both modeling and data analysis. Improved estimates of CRF were obtained based on precise space and time collocated ground and satellite measurement of broadband (BB) shortwave (SW) fluxes. Pixel level Earth Radiation Budget Experiment (ERBE), scanner for radiation budget (ScaRaB), and Clouds and Earth's Radiant Energy (CERES) experiment satellite data were matched to observations at several Canadian radiation stations, the Atmospheric Radiation Measurement (ARM) central facility site in central Oklahoma, SURFRAD (National Oceanic and Atmospheric Administration [NOAA]), and Baseline Surface Radiation Network (BSRN) (World Meteorological Organization [WMO]) stations during 1988-1990, 1994-1995, and 1998. The results obtained show the CRF ratio falls within 0.88-1.17, which implies approximately the same magnitude of atmospheric absorption under clear-sky and cloudy-sky conditions.

Basic Definitions

Lets denote net flux at the top of (the) atmosphere (TOA) (surface) level as T(S) = $F^{T(S)}\downarrow - F^{T(S)}\uparrow = \left(1-\alpha^{T(S)}\right)F^{T(S)}\downarrow$, then CRF is $C^{T(S)} = T(S) - T(S)^{CLR}$, where $\alpha^{T(S)}$ is surface TOA albedo. Index "CLR" denotes the clear-sky scene. To estimate the mean effect of clouds on energy balance, average quantities are employed

$$C^{T(S)} = \frac{1}{N}\sum_i \left(T(S)_i - T(S)_i^{CLR}\right) \quad (1)$$

The quantities T,T^{CLR} and S,S^{CLR} cannot be derived from real observations simultaneously for each observational moment "I". They are available either at clear-sky conditions or "not clear-sky conditions" (cloudy, partly cloudy, etc). Instead of Eq. (1), the "observational" average cloud radiative forcing is often used

$$O^{T(S)} = \frac{1}{N}\sum_i T(S)_i - \frac{1}{N_{CLR}}\sum_{i\in CLR} T(S)_i^{CLR} \quad (2)$$

The difference between "observed" and "required" cloud radiative forcing is:

$$\Delta^{T,S} = C^{T,S} - O^{T,S} = (1 - p_{CLR})\left(\Psi^{T,S} - \Omega^{T,S}\right),$$

where p_{CLR} is a probability of clear-sky scene,

$\Psi^{T,S} = \frac{1}{N_{CLR}}\sum_{i\in CLR} T(S)^{CLR}$ is observed clear-sky offset, and

$\Omega^{T,S} = \frac{1}{N_{NCLR}}\sum_{i\in NCLR} T(S)^{CLR}$ is hypothetical clear-sky offset for scenes with clouds.

Cloud radiative forcing ratio R is thus given by:

$$R = \frac{C^S}{C^T} = \frac{O^S + \Delta^S}{O^T + \Delta^T} \approx \tilde{R} + \frac{\Delta^S}{\Delta^T} - \tilde{R}\frac{\Delta^T}{O^T}, \quad (3)$$

where $\tilde{R}$ is observed CRF ratio: $\tilde{R} = \frac{\Delta^S}{O^T}$. Therefore, the difference $\Delta R = R - \tilde{R}$ is not equal to zero unless the hypothetical clear-sky offset for cloudy scenes in Eq. (1) is equal to the average clear-sky offset for clear-sky scenes in Eq. (2). These two factors may differ from each other due to differences in atmospheric state. Most important differences are associated with water vapor and aerosol loading.

Model Simulations

Aerosol Effect

The modeled results for CRF ratio R due to different aerosol loadings for the continental aerosol are presented in Figure 1. The difference in aerosol amount between two atmospheric states causes correction to cloud radiative forcing. Surface net flux is more sensitive to variations in aerosol than TOA flux is, since aerosol absorption and scattering have opposite effects for TOA fluxes, while they have the same attenuation effect for surface net flux. The corrections shown in Figure 1 are defined relative to the basic clear-sky state with difference in aerosol optical thickness $\Delta\tau_a$ = 0.1, 0.2, 0.3. The magnitude of the correction ΔR increases with $\Delta\tau_a$ and solar zenith angle (SZA) and decreases with sun elevation. The correction is always positive, because a lower aerosol loading was assumed for the basic atmospheric state. The correction may become rather significant, for strong absorbing aerosol of large loading such as smoke aerosols.

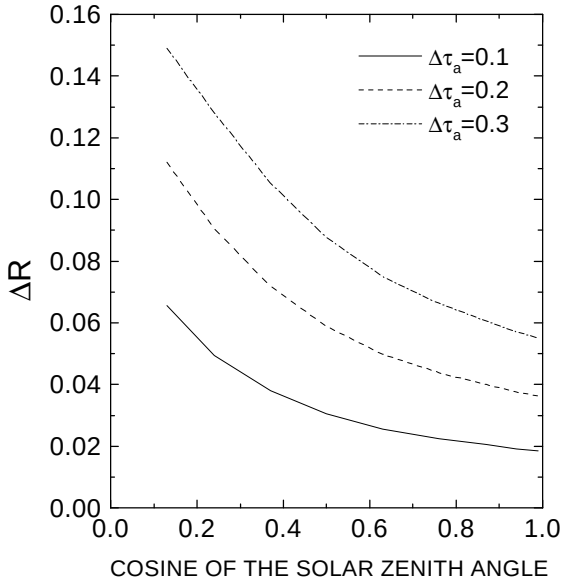

Figure 1. Correction to CRF ratio R due to aerosol mismatch between clear-sky scenes and scenes with clouds.

Water Vapor Effect

The effect of water vapor on cloud forcing ratio is more pronounced than that of aerosol, as is shown in Figure 2, due to its predominant absorbing effect. Unlike aerosol, the TOA radiative forcing due to water vapor at the TOA is positive, meaning smaller TOA albedo for larger precipitable water vapor in the atmosphere. The magnitude of the TOA forcing is again less than at the surface. Due to saturation of absorption of SW radiation by water vapor, the effect of unequal water vapor amounts under clear-sky and cloudy conditions is more important for drier atmosphere. The correction in observed CRF ratio ΔR may be as much as 0.15 to 0.2 for a difference of 1 cm in water vapor content.

Determination of CRF Ratio

Ground radiation measurements used here were collected under various observation programs. They include the Canadian observational network operated by the Atmospheric Environment Service of Canada (Barker et al. 1998); the NOAA's SURFRAD network (DeLuisi et al. 1996); the WMO's BSRN (Ohmura et al. 1998); and the U.S. Department of Energy's ARM Program (Michalsky et al. 1999). Satellite measurements made by ERBE, ScaRaB, and CERES were used in combination with ground observations. ERBE data are from 1988 to 1990, ScaRaB data for 1994-1995, and CERES data for 1998. All analyses are limited to snow-free scenes, as determined by satellite scene identification with surface type flagged as snow/ice free. We applied the algorithm of Li and Garand (1994) to retrieve clear-sky surface albedo from satellite measurements.

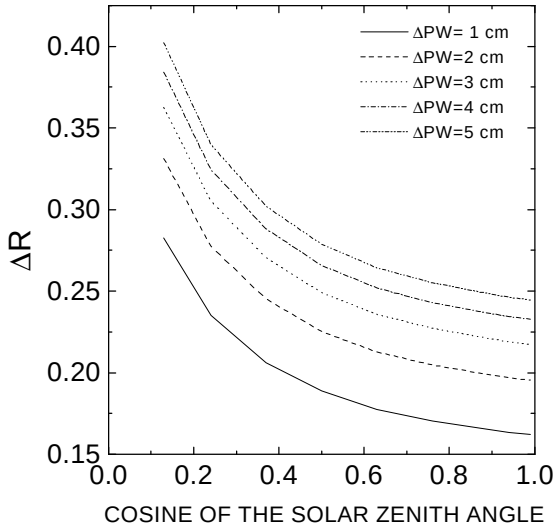

Figure 2. Correction to cloud radiative forcing due to water vapor mismatch.

Only the data with simultaneous satellite and ground observations were used in estimating the solar net fluxes at TOA and surface. The distance between centers of satellite ERBE/ScaRaB pixel and station location is less that 20 km, approximately half-pixel size for ERBE/ScaRaB data. For CERES data, the distance is limited to 10 km. Only data points with satellite pixel geotype corresponding to "land" were used for subsequent analysis. 30-minute average values were used as ground measurements.

To identify clear-sky offset, we applied two independent methods. The first method is similar to the method of Chou and Zhao (1997). It employs the following constraints:

1. Satellite scene is identified as "clear over land."

2. Standard deviation of ground direct flux $\sigma_{Dir} < 20$ W/m^2 and of diffuse flux $\sigma_{Dif} < 7$ W/m^2 during a 30-minute interval.

3. The ratio Dif/Total is less than 0.6.

The above preliminary tests remove bulk clouds, but the selected data may still be contaminated by residual clouds. A further test is applied to direct fluxes. For the selected data, direct fluxes are fitted with a third-order polynomial F^{DIR}_{appr} with respect to μ and the standard deviation σ_{DIR} of the residuals are computed. Data satisfying the following condition are removed.

$$(F^{DIR}_{appr} - F^{DIR}) < (\sigma_{DIR} + \sigma_{DIR} * \mu).$$

The example of preliminary selected fluxes and 1 step iteration is shown in Figure 3 for Winnipeg. Analysis of direct and diffuse components shows that this identification of clear-sky points is quite

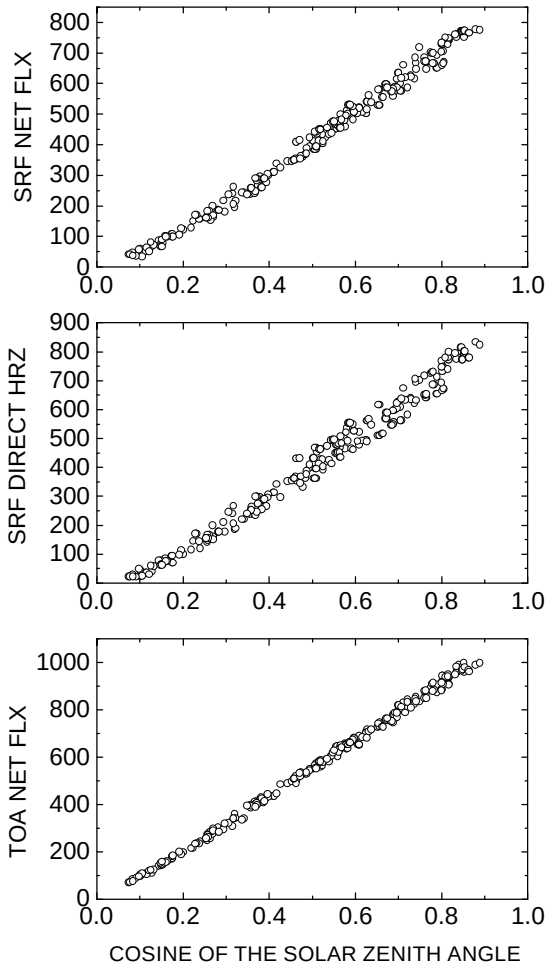

Figure 3. Clear-sky points after 1 step iteration in selection procedure. Winnipeg. ERBE data for 1988-1990.

reliable. The first iteration removes all cloud-contaminated data. Further iterations increase clear-sky reference by removing the data of larger aerosol and water vapor loading, thereby increasing the magnitude of cloud radiative forcing at the surface, according to Eq. (3) and modeling results of the section above on "Modeling Simulations." Influence of number of iterations used to select the subset of clear-sky points is demonstrated in Figure 4.

The second method for determining clear-sky offset is to establish a climatological relationship between clear-sky fluxes and the influencing factors. Assuming that aerosol loadings for clear and cloudy conditions are the same, we may parameterize clear-sky fluxes as a function of water vapor amount and SZA. The "clear-sky" reference values for cloudy measurements can then be derived from the corresponding perceptible water and SZA. To this end, we processed all available ground measurements for each station and applied clear-sky identification approach similar to the one proposed by Long and Ackerman (1996). Clear-sky intervals were identified according to the minimal values of diffuse radiation and approximation of logarithms of total/diffuse ratio and flux components by quadratic

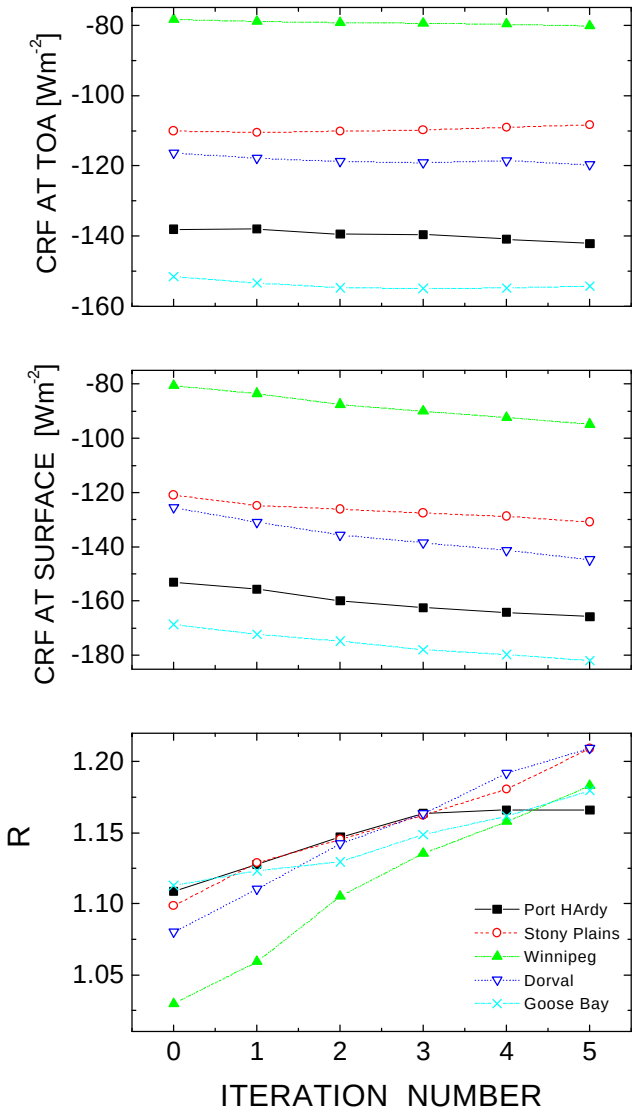

Figure 4. Cloud radiative forcing for different number of iterations used to establish clear-sky offset.

polynomials with respect to the cosine of the SZA. The average fluxes were obtained for each precipitable water bin of 0.25 cm and cosine of SZA bin of 0.05. Intermediate values were derived by interpolation. Precipitable water vapor amounts were taken from the National Center for Atmospheric Research (NCAR)/NOAA REANALYSIS data set (Kalnay et al. 1996). Only the results of identification with more than 3 hours of clear skies per day were included in the computation of clear-sky average values.

Cloud Radiative Forcing from ERBE, ScaRaB, and CERES Data

The estimates of CRF and CRF ratio are presented in Tables 1 and 2 for 10 and 6 radiation stations. Table 1 contains the results obtained by the first method of clear-sky detection, while Table 2 includes the results for method 2. The number of stations is less in Table 2 because not all the data had the detailed information about all components of surface radiative fluxes necessary to identify cloudy free intervals and compute clear-sky means. Based on two different independent methods of clear-sky offset determination, our analysis shows very moderate influence of cloud on absorption of solar radiation in the atmosphere. CRF values vary from 0.88 to 1.17, being mostly between 0.98 and 1.1. We studied the sensitivity of CRF ratio to the magnitude of surface albedo by changing albedo values ±0.03. This variation causes ±0.05 change in the magnitude of R.

Table 1. Cloud radiative forcing from ERBE, ScaRaB, and CERES (method 1).

	ERBE			ScaRaB			CERES		
	R	**CRF_S**	**CRF_{TOA}**	**R**	**CRF_S**	**CRF_{TOA}**	**R**	**CRF_S**	**CRF_{TOA}**
1. Port Hardy (AES)	1.13	-155.6	-138.0	1.03	-166.8	-162.3	--	--	--
2. Stony Plains (AES)	1.13	-124.8	-110.5	1.10	-121.7	-110.9	--	--	--
3. Winnipeg (AES)	1.06	-83.6	-78.9	1.00	-122.5	-122.5	--	--	--
4. Dorval (AES)	1.11	-130.9	-117.9	1.02	-152.1	-149.9	--	--	--
5. Goose Bay (AES)	1.12	-172.2	-153.3	0.97	-172.7	-177.4	--	--	--
6. DOE ARM SGP CF (Oklahoma)	--	--	--	1.07	-95.30	-89.3	1.05	-93.4	-89.7
7. Boulder (SURFRAD)	--	--	--	0.89	-107.7	-120.9	1.02	-109.3	-106.3
8. Bondville (SURFRAD)	--	--	--	--	--	--	0.88	-151.7	-163.1
9. Goodween Creek (SURFRAD)	--	--	--	--	--	--	1.10	-128.2	-116.8
10. Payerne (BSRN)	--	--	--	0.91	-123.2	-135.7			

Table 2. Cloud radiative forcing obtained by alternative method where surface clear-sky offset derived as climatic mean (method 2).

	ERBE			ScaRaB			CERES		
	R	**CRF_S**	**CRF_{TOA}**	**R**	**CRF_S**	**CRF_{TOA}**	**R**	**CRF_S**	**CRF_{TOA}**
1. Port Hardy (AES)	1.17	-173.2	-147.6	1.11	-185.8	-167.4	--	--	--
2. Stony Plains (AES)	1.07	-122.1	-114.1	1.14	-143.5	-125.7	--	--	--
3. Winnipeg (AES)	1.04	-85.2	-81.6	1.01	-128.1	-126.7	--	--	--
4. Dorval (AES)	1.04	-126.3	-120.7	1.01	-149.7	-148.7	--	--	--
5. DOE ARM SGP CF (Oklahoma)	--	--	--	0.98	-88.2	-90.1	1.00	-92.4	-92.1
6. Payerne (BSRN)	--	--	--	0.97	-150.6	-154.4			

Separate analysis of clear-sky and cloudy scenes showed also that for Canadian stations for ScaRaB and ERBE data both surface measured and satellite retrieved values of downward flux are in good agreement. This is consistent with Jing and Cess (1998), but their study is restricted to clear-sky only. However, there is a noticeable overestimation of clear-sky fluxes retrieved from satellite for ARM and a

few other sites. The difference is most significant for retrievals employing CERES data. One of the factors contributing to this discrepancy is the systematic difference noticed in clear-sky mean fluxes between the measurements made by different kinds of radiometers. Better treatment of aerosol effects and understanding of uncertainties in routine measurements of broadband solar radiative fluxes are needed to resolve existing questions.

Conclusions

The study demonstrates the sensitivity of the determination of cloud radiative forcing and its ratio at the surface versus TOA to the fluctuations in atmospheric state between clear and cloudy conditions, especially for water vapor and aerosol.

The estimates of CRF and CRF ratio are obtained from extensive ground and satellite observations from ERBE, ScaRaB, and CERES. Derived values of CRF show a very moderate influence of cloud on absorption of solar radiation in the atmosphere. CRF values vary from 0.88 to 1.17, being mostly within 0.98 and 1.1.

References

Barker, H. W, T. J. Curtis, E. Leontieva, and K. Stamnes, 1998: Optical depth of overcast cloud across Canada: Estimates based on surface pyranometer and satellite measurements. *J. Clim.*, **11**, 2980-2994.

Chou, M.-D., and W. Zhao, 1997: Estimation and model validation of surface solar radiation and cloud radiative forcing using TOGA COARE measurements. *J. Clim.*, **10**, 610-620.

DeLuisi, J. J., J. A. Augustine, E. C. Weatherhead, B. Hicks, D. Matt, and C. V. Alonso, 1996: The GCIP Surface Radiation Budget Network (SURFRAD). Preprint Volume, *Second International Scientific Conference on the Global Energy and Water Cycle*, June 17-21, 1996. Washington, D.C., pp. 407-408.

Jing, X., and R. D. Cess, 1998: Comparison of atmospheric clear-sky shortwave radiation models to collocated satellite and surface measurements in Canada. *J. Geophys. Res.*, **103**, 28,817-28,825.

Kalnay, E., M. Kanamitsu, R. Kisler, W. Collins, D. Deaven, L. Gandin, M. Iredell, S. Sasha, G. White, J. Woolen, Y. Zhu, M. Chelliah, W. Ebisuzaki, W. Higgins, J. Janowiak, K. C. Mo, C. Ropelewski, J. Wang, A. Leetmaa, R. Reynolds, R. Jenne, and D. Joseph, 1996: The NCEP/NCAR 40-year reanalysis project. *Bull. Amer. Meteor. Soc.*, **77**, 437-471.

Li, Z., and L. Garand, 1994: Estimation of surface albedo from space: A parameterization for global application. *J. Geophys. Res.*, **99**, 8335-8350.

Long, C. N., and T. P. Ackerman, 1996: Detection of clear skies using total and diffuse shortwave irradiance: Calculations of shortwave cloud radiative forcing and clear-sky diffuse ratio. In *Proceedings of the Sixth Atmospheric Radiation Measurement (ARM) Science Team Meeting*, CONF-9603149, pp. 179-183. U.S. Department of Energy, Washington, D.C.

Michalsky, J., E. Dutton, M. Rubes, D. Nelson, T. Stoffel, M. Wesley, M. Splitt, and J. DeLuisi, 1999: Optimal measurement of surface shortwave irradiance using current instrumentation. *J. Atmos. Ocean. Tech*., **16**, 55-69.

Ohmura A. et al., 1998: Baseline Surface Radiation Network (BSRN/WRMC), a new precision radiometry for climate research. *Bull. Amer. Meteor. Soc*., **79**, 2115-2136.